SIAM J. Appl. Math.
Vol. 75, No. 1, pp. 189–208

HIGH-ORDER DAVIES' APPROXIMATION FOR A SOLITARY WAVE SOLUTION IN PACKHAM'S COMPLEX PLANE*

SUNAO MURASHIGE† AND WOOYOUNG CHOI‡

Abstract. This paper considers a progressive solitary wave of permanent form in an ideal fluid of constant depth and explores Davies' approximation [*Proc. R. Soc. Lond. A*, 208 (1951), pp. 475–486] with high-order corrections to Levi-Civita's surface condition for the logarithmic hodograph variable. Using a complex plane that was originally introduced by Packham [*Proc. R. Soc. Lond. A*, 213 (1952), pp. 234–249], it is shown that a singularity at infinity can be regularized. Therefore, the solutions in Packham's complex plane under high-order Davies' approximation maintain two critical properties of a solitary wave, the correct exponential decay in the outskirt of wave and the harmonic property of a solution, that are often violated in classical long wave approximations. After introducing an accurate numerical method to compute solitary wave solutions in Packham's complex plane, we compare high-order Davies' approximate solutions with fully nonlinear solutions as well as long wave approximate solutions. The results demonstrate that high-order Davies' approximation produces rapidly converging series solutions even for relatively large amplitude waves and that Davies' approximate solutions compare much better with the fully nonlinear solutions than the long wave approximate solutions.

Key words. solitary waves, gravity water waves, approximation in the complex domain

AMS subject classifications. 30E10, 76B15, 76B25

DOI. 10.1137/140980843

1. Introduction.

In this work, we study two-dimensional irrotational motion of a solitary wave progressing in permanent form on a layer of water of constant depth h with constant wave speed c, assuming that the fluid is incompressible and inviscid. In the frame of reference moving with wave speed c, the wave becomes steady and the free surface is represented by the streamline of $\psi = 0$. This problem can be formulated in the complex velocity potential f $(= \phi + \mathrm{i}\psi)$-plane using the logarithmic hodograph variable $\omega = \tau + \mathrm{i}\theta = \log(c/w)$ as a flow variable, where $w = \mathrm{d}f/\mathrm{d}z = u - \mathrm{i}v = q\mathrm{e}^{-\mathrm{i}\theta}$ is the complex velocity, $q = \sqrt{u^2 + v^2}$, and $z = x + \mathrm{i}y$ is the complex coordinate. The free surface condition for the logarithmic hodograph variable ω can be written in the form of Levi-Civita's surface condition [16, section 14.65]:

$$\frac{\partial \tau}{\partial \phi} - \frac{1}{F^2}\mathrm{e}^{3\tau}\sin\theta = 0 \quad \text{on} \quad \psi = 0, \tag{1.1}$$

where $F = c/\sqrt{gh}$ is the Froude number and g denotes the gravitational acceleration. Notice that the form of (1.1) is slightly different from that in [16, section 14.65] because the definition of the logarithmic hodograph variable $\omega = \tau + \mathrm{i}\theta$ follows that of [26].

Due to the highly nonlinear nature of the free surface boundary condition (1.1), a long wave approximation is often adopted to obtain analytically solitary wave solutions, for which the variation of a flow is assumed slow in the horizontal direction.

*Received by the editors August 4, 2014; accepted for publication (in revised form) December 16, 2014; published electronically February 12, 2015.
http://www.siam.org/journals/siap/75-1/98084.html
†Department of Mathematics and Informatics, Ibaraki University, Mito, Ibaraki, 310-8512, Japan (murasige@mx.ibaraki.ac.jp).
‡Department of Mathematical Sciences, New Jersey Institute of Technology, Newark, NJ 07102-1982 (wychoi@njit.edu). The work of this author was supported by the Korean Federation of Science and Technology Societies through the Brain Pool Program, grant 141S-2-3-0002.

Then, dependent variables are expanded around the bottom in Taylor series, and high-order derivative terms in the horizontal direction are neglected. The leading-order truncation of the series yields a classical long wave approximate equation, often in the form of an ordinary differential equation, for a dependent variable evaluated at the bottom. Friedrichs and Hyers [8] applied this approximation for ω to Levi-Civita's surface condition to prove the existence of a solitary wave solution. The weakly nonlinear assumption is often combined with the long wave approximation [7, 8, 11, 14, 20] but can be avoided, as shown by Lord Rayleigh [12, section 252], [23]. In his seminar work, Lord Rayleigh [23] first derived an approximate equation for solitary waves without the small amplitude assumption and found a better relationship between wave speed and wave amplitude than the weakly nonlinear result from the KdV equation [11]. The order of approximation can be increased with the order of truncation of the series, and high-order long wave approximate solutions have been studied by various authors [7, 14, 15, 20, 21, 27]. Unfortunately, since a corner develops at the crest as the wave amplitude approaches its maximum value, convergence of the series becomes slower with the increase of wave amplitude. Therefore, some acceleration techniques such as the Padé approximants or the Shanks transformation are required for steep solitary waves.

In addition to its slow convergence, another difficulty in using the long wave approximation to compute a steady solitary wave solution lies in the exponential decay in the outskirt of solitary wave. Friedrichs and Hyers [8, p. 518] pointed out that this decay property causes the nonuniform convergence of the wave elevation to a flat water surface with the decrease of wave amplitude and prevents one from approximating solitary waves from periodic waves. Stokes [12, section 252], [22] found the exponential decay of a solution using the linearized free surface condition that is valid in the outskirt. He showed that solitary wave solutions exponentially decay with the factor $\mathrm{e}^{-\mu\pi|x|/h}$ as the horizontal coordinate x tends to $\pm\infty$, and the decay rate μ is related to the Froude number F by

$$1/F^2 = \mu\pi \cot \mu\pi, \tag{1.2}$$

which is called Stokes' relation in this paper. Byatt-Smith proved using an exact integral equation in the appendix of his paper [1] that all solitary wave solutions satisfy this decay condition and the decay rate μ is the smallest positive root of (1.2). Although it has been directly incorporated in the fully nonlinear computations of steady solitary waves [6, 10, 13, 15, 26, 28], [25, section 6], this exponential decay condition (1.2) is violated in long wave approximate solutions. Furthermore, the truncation of the long wave expansion destroys the harmonic property of a solution. Here the harmonic property means that the dependent complex variable is regular, and its real and imaginary parts satisfy Laplace's equations. Therefore, the long wave approximation becomes inaccurate with the increase of wave amplitude and it would be useful to adopt a new approximate method to obtain more reliable solutions for relatively large amplitude solitary waves.

An alternative approximation to Levi-Civita's surface condition (1.1) was made by Davies [3, 4], who approximated $\sin\theta$ by $(1/3)\sin 3\theta$, where $\theta = \arctan(v/u)$ on the free surface. We call this Davies' approximation. It was then shown that closed-form solutions for the approximate condition can be found for periodic waves in water of infinite and finite depth. For shallow water, under Davies' approximation, Packham [19] obtained analytically a steady solitary wave solution in a complex plane. In this Packham's complex plane, the flow domain is conformally mapped and a singularity at

infinity connected with the exponential decay of a steady solitary wave [28] is removed. Therefore, a solitary wave solution is analytic in the domain and on its boundary (as also shown in section 3). Davies' approximation can be further improved with high-order corrections to the approximation of $\sin\theta$ in Levi-Civita's surface condition (1.1), but no attempts have been made yet to obtain high-order solitary wave solutions or examine their convergence to the fully nonlinear solutions.

In this paper, we consider a high-order Davies' approximation of Levi-Civita's surface condition (1.1) to find a steady solitary wave solution in Packham's complex plane. It is shown that the solution expanded in the form of power series is regular and satisfies the exponential decay property with Stokes' relation (1.2) exactly. By using a numerical method, where convergence of the series is optimized using an orthogonalized polynomial system, high-order Davies' approximation is found to produce rapidly converging series solutions even for relatively large amplitude waves.

The paper is organized as follows. The problem is formulated using the logarithmic hodograph variable ω, and high-order Davies' approximation of Levi-Civita's surface condition is presented in section 2. After it is shown that the exponential decay of a solution in the outskirt of wave is related to a singularity of a solution for ω, Packham's complex plane is introduced in section 3 to regularize the problem. Using the method described in section 4, solitary wave solutions under high-order Davies' approximation are computed and are then compared with fully nonlinear solutions as well as solutions of the weakly and strongly nonlinear long wave equations.

2. Formulation of the problem.

2.1. Formulation using the logarithmic hodograph variable in the complex velocity potential plane. Consider a left-going solitary wave in the frame of reference moving with wave speed c, as shown in Figure 1(a), in which the wave is steady and bounded above by its free surface and below by the horizontal bottom in the (x,y)-plane. Assume that the flow is irrotational and that the fluid is incompressible and inviscid. Then we can represent this irrotational plane flow using the logarithmic hodograph variable ω defined by

$$\omega = \tau + \mathrm{i}\theta = \log(c/w) \quad \text{with} \quad \tau = \log(c/q) \quad \text{and} \quad \theta = \arctan(v/u), \tag{2.1}$$

where $w = \mathrm{d}f/\mathrm{d}z = u - \mathrm{i}v$ is the complex velocity, $f = \phi + \mathrm{i}\psi$ is the complex velocity potential, $z = x + \mathrm{i}y$, and $q = \sqrt{u^2 + v^2}$. With the length scaled by the depth h and the velocity by the wave speed c, we have the following dimensionless variables:

$$\alpha = a/h\ , \quad z_* = z/h\ , \quad f_* = f/(ch)\ , \quad w_* = w/c, \quad \text{and} \quad q_* = q/c, \tag{2.2}$$

where a denotes the wave amplitude. Hereafter the asterisks in (2.2) are omitted for brevity.

It is convenient to formulate this two-dimensional steady problem in the complex velocity potential f-plane, where the flow domain is mapped onto the infinite strip $-1 \le \psi \le 0$ and $-\infty < \phi < \infty$, as shown in Figure 1(b), because the free surface is on the streamline $\psi = 0$ in the f-plane. The free surface condition in the f-plane is given by Bernoulli's equation:

$$\frac{1}{2}q^2 + \frac{1}{F^2}y = \text{constant} \quad \text{on} \quad \psi = 0. \tag{2.3}$$

Taking differentiation of this with respect to ϕ, we can obtain Levi-Civita's surface condition [16, section 14.65] given by (1.1). The bottom boundary condition $v = 0$

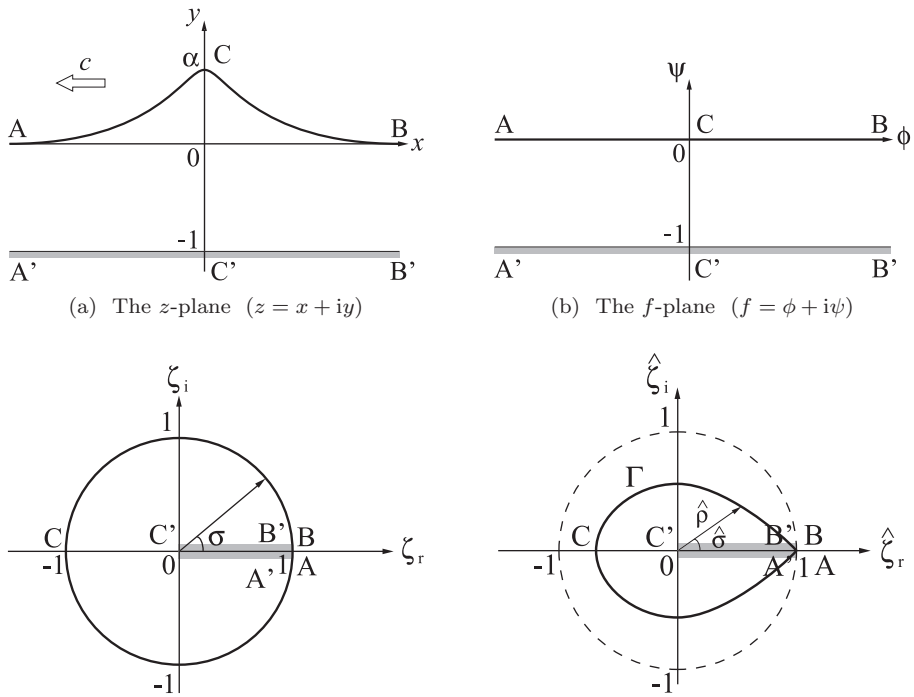

(a) The z-plane $(z = x + \mathrm{i}y)$ (b) The f-plane $(f = \phi + \mathrm{i}\psi)$

(c) The ζ-plane $(\zeta = \zeta_\mathrm{r} + \mathrm{i}\zeta_\mathrm{i})$ (d) The $\hat{\zeta}$-plane $(\hat{\zeta} = \hat{\zeta}_\mathrm{r} + \mathrm{i}\hat{\zeta}_\mathrm{i})$

FIG. 1. *Conformal mapping of the flow domain of a solitary wave. The length and the velocity are scaled by the water depth h and the wave speed c, respectively.* Γ*: the free surface given by* $\hat{\zeta} = \hat{\rho}(\hat{\sigma})\mathrm{e}^{\mathrm{i}\hat{\sigma}}$ *in the* $\hat{\zeta}$*-plane.*

at $y = -1$ or $\psi = -1$ and the infinity condition $w \to 1$ as $x \to \pm\infty$ or $\phi \to \pm\infty$ are given by

$$\theta = 0 \quad \text{on} \quad \psi = -1 \quad \text{and} \quad -\infty < \phi < \infty \tag{2.4}$$

and

$$\omega = \tau + \mathrm{i}\theta \;\to\; 0 \quad \text{as} \quad \phi \to \pm\infty, \tag{2.5}$$

respectively. In addition, assuming that the wave profile is symmetric with respect to the vertical line $x = 0$ or $\phi = 0$ at the crest, we have another condition given by

$$\theta = 0 \quad \text{on} \quad \phi = 0 \quad \text{and} \quad -1 \le \psi \le 0. \tag{2.6}$$

From these, the problem in the f-plane is to find an analytic function $\omega = \omega(f)$ satisfying the conditions (1.1), (2.4), (2.5), and (2.6).

2.2. Davies' approximate surface condition. When the wave slope is small, namely, for small values of $|\theta|$, the term $\sin\theta$ in Levi-Civita's surface condition (1.1) can be approximated as

$$\sin\theta \;\sim\; \frac{1}{3}\sin 3\theta. \tag{2.7}$$

Then the approximate surface condition can be expressed as

$$\frac{\partial \tau}{\partial \phi} - \frac{1}{3F^2}\mathrm{e}^{3\tau}\sin 3\theta = 0 \quad \text{or} \quad \mathrm{Re}\left\{\frac{\mathrm{d}\omega}{\mathrm{d}f} + \mathrm{i}\frac{1}{3F^2}\mathrm{e}^{3\omega}\right\} = 0 \qquad \text{on} \;\; \psi = 0. \tag{2.8}$$

Davies applied this approximation to periodic waves on water of infinite depth [3] [16, section 15.59] and finite depth [4], while Packham [19] obtained a solitary wave solution in a complex plane described in the subsequent section.

Davies' approximation (2.8) to Levi-Civita's surface condition (1.1) can be improved. From $\sin\theta = \frac{1}{3}\sin 3\theta + \frac{4}{3}\sin^3\theta$, a higher-order approximation of $\sin\theta$ can be found as [3, 18]

$$\sin\theta \;\sim\; \sum_{m=1}^{M} A_m (\sin 3\theta)^{2m-1} \tag{2.9}$$

with

$$A_1 = 1/3 \;\text{ and }\; A_m = \frac{4}{3}\sum_{i=1}^{m-1}\left\{A_{m-i}\left(\sum_{j=1}^{i} A_j A_{i+1-j}\right)\right\} \qquad (m = 2, \ldots, M), \tag{2.10}$$

where $A_2 = 4/81, A_3 = 16/729, \ldots$. This approximation is in principle valid for relatively small wave slope, i.e., $|\theta|$ less than about $\pi/6$, but its applicability to relatively large amplitude waves will be examined later in comparison with fully nonlinear solutions.

Davies [3] obtained high-order approximate solutions for periodic waves on water of infinite depth using (2.9) with $M = 2$ and 3, but no high-order approximate solitary wave solutions using (2.9) for $M \geq 2$ have been obtained yet.

3. Packham's complex plane.

3.1. A singularity of a solitary wave solution at infinity. Conformal mapping of the flow domain onto the unit disk $|\zeta| < 1$ in the ζ-plane shown in Figure 1(c) helps us examine the decay property of a solitary wave solution in its outskirt and derive Packham's complex plane in section 3.2. The f-plane is mapped onto the ζ-plane by

$$\zeta = \tanh^2\left\{\frac{\pi}{4}(f + \mathrm{i})\right\} \quad \text{or} \quad f + \mathrm{i} = \frac{2}{\pi}\log\left(\frac{1+\sqrt{\zeta}}{1-\sqrt{\zeta}}\right), \tag{3.1}$$

where the log function and $\sqrt{\zeta}$ are uniquely defined with the branch cut along the positive ζ-axis ($0 \leq \zeta \leq 1$). In the ζ-plane, the free surface is mapped onto $\zeta = \mathrm{e}^{\mathrm{i}\sigma}$ ($0 < \sigma < 2\pi$), and the points at infinity, namely, A, A$'$, B, and B$'$ in Figure 1, are mapped onto $\zeta = 1$. Since (3.1) gives $\partial\phi/\partial\sigma = -1/\{\pi\sin(\sigma/2)\}$ on the free surface $\zeta = \mathrm{e}^{\mathrm{i}\sigma}$, Levi-Civita's surface condition (1.1) is expressed in the ζ-plane as

$$\pi\sin\frac{\sigma}{2}\,\frac{\partial\tau}{\partial\sigma} + \frac{1}{F^2}\mathrm{e}^{3\tau}\sin\theta = 0 \quad \text{on} \;\; \zeta = \mathrm{e}^{\mathrm{i}\sigma} \quad (0 < \sigma < 2\pi). \tag{3.2}$$

For convenience, we write a solution ω in the ζ-plane as $\omega = \omega(\zeta)$, instead of $\omega = \omega(f(\zeta))$. From the infinity condition $\omega(\zeta) \to 0$ as $\zeta \to 1$ and the bottom condition $\theta = 0$ on $0 \leq \zeta \leq 1$, we can assume $\omega(\zeta) \sim d_0(1-\zeta)^p$ as $\zeta \to 1$, where d_0 and p are real constants and $p > 0$. Then, on the free surface $\zeta = \mathrm{e}^{\mathrm{i}\sigma}$, $\tau(\sigma) \sim d_0\cos(p\pi/2)\cdot\sigma^p$,

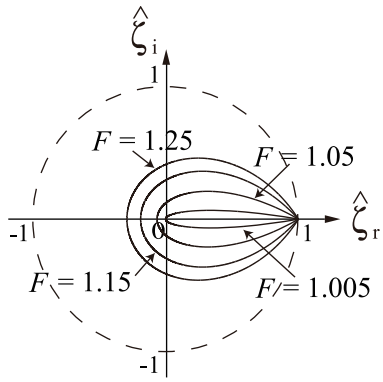

FIG. 2. *The free surface* Γ *for different values of the Froude number* F *in the* $\hat{\zeta}$*-plane* ($\hat{\zeta} = \hat{\zeta}_r + i\hat{\zeta}_i$). *Broken line: a unit circle.*

and $\theta(\sigma) \sim -d_0 \sin(p\pi/2) \cdot \sigma^p$ as $\sigma \to 0$, where $\sigma = 0$ corresponds to the physical infinity $\zeta = 1$. Substituting these into the free surface condition (3.2) and equating the coefficients of σ^p for small σ, we get $p = 2\mu$, namely,

$$\omega(\zeta) \sim d_0 (1-\zeta)^{2\mu} \qquad \text{as } \zeta \to 1, \tag{3.3}$$

where μ satisfies Stokes' relation (1.2) [1], [12, section 252], [22]. Thus $\omega = \omega(\zeta)$ has a branch point type singularity at $\zeta = 1$ which is connected with the exponential decay of a solitary wave solution in the outskirt.

3.2. Regularization of the singularity at infinity using conformal mapping. It is not straightforward to represent a solitary wave solution in the form of convergent series in the ζ-plane due to the singularity at infinity or at $\zeta = 1$ in (3.3). In order to regularize this singularity, Packham [19] introduced a complex variable $\hat{\zeta}$ defined by

$$\hat{\zeta} = \tanh^2\left\{\frac{\mu\pi}{2}(f + i)\right\} \quad \text{or} \quad f + i = \frac{1}{\mu\pi}\log\left(\frac{1+\sqrt{\hat{\zeta}}}{1-\sqrt{\hat{\zeta}}}\right), \tag{3.4}$$

where μ is the smallest positive root of Stokes' relation (1.2), as described in section 1. This transformation conformally maps the flow domain onto the inside of the closed curve Γ in the $\hat{\zeta}$-plane, as shown in Figure 1(d). The closed curve Γ corresponds to the free surface and can be written in the polar coordinate form $\hat{\zeta} = \hat{\rho}(\hat{\sigma})e^{i\hat{\sigma}}$ with

$$\hat{\rho}(\hat{\sigma}) = \left(-\sin\frac{\hat{\sigma}}{2} + \sqrt{\sin^2\frac{\hat{\sigma}}{2} + \tan^2\mu\pi}\right)^2 \Big/ \tan^2\mu\pi. \tag{3.5}$$

Thus the crest C is mapped onto $\hat{\zeta} = -\hat{\rho}(\pi) = -\tan^2(\mu\pi/2)$, and the shape of the closed curve Γ in the $\hat{\zeta}$-plane depends on μ or the Froude number F, as shown in Figure 2. Similarly to the ζ-plane, we write a solution ω in the $\hat{\zeta}$-plane as $\omega = \omega(\hat{\zeta})$, instead of $\omega = \omega(f(\hat{\zeta}))$, and ω on the free surface Γ as $\omega(\hat{\zeta} = \hat{\rho}(\hat{\sigma})e^{i\hat{\sigma}}) = \tau(\hat{\sigma}) + i\theta(\hat{\sigma})$.

From (3.4) and (3.5), $\partial\phi/\partial\hat{\sigma}$ on the free surface $\hat{\zeta} = \hat{\rho}(\hat{\sigma})\mathrm{e}^{\mathrm{i}\hat{\sigma}}$ can be written as

$$\frac{\partial\phi}{\partial\hat{\sigma}} = -\frac{(\tan\mu\pi/\mu\pi)}{2\sin\dfrac{\hat{\sigma}}{2}\sqrt{\sin^2\dfrac{\hat{\sigma}}{2}+\tan^2\mu\pi}} = -\frac{F^2}{2\sin\dfrac{\hat{\sigma}}{2}\sqrt{\sin^2\dfrac{\hat{\sigma}}{2}+\tan^2\mu\pi}}, \tag{3.6}$$

where Stokes' relation (1.2) is used. Then the free surface condition for $\tau = \tau(\hat{\sigma})$ and $\theta = \theta(\hat{\sigma})$ in the $\hat{\zeta}$-plane can be expressed as

$$G(\hat{\sigma}) := 2\sin\frac{\hat{\sigma}}{2}\sqrt{\sin^2\frac{\hat{\sigma}}{2}+\tan^2\mu\pi}\,\frac{\partial\tau}{\partial\hat{\sigma}} + \mathrm{e}^{3\tau}\sin\theta = 0 \quad \text{on } \hat{\zeta} = \hat{\rho}(\hat{\sigma})\mathrm{e}^{\mathrm{i}\hat{\sigma}} \quad (0 < \hat{\sigma} < 2\pi). \tag{3.7}$$

This is Levi-Civita's surface condition in the $\hat{\zeta}$-plane. The points at infinity A, A′, B, and B′ are mapped onto $\hat{\zeta} = 1$. From (3.1), (3.3), and (3.4), we can find

$$\omega(\hat{\zeta}) \sim \hat{d}_0\,(1-\hat{\zeta}) \qquad \text{as } \hat{\zeta} \to 1, \tag{3.8}$$

where $\hat{d}_0$ is a real constant. Thus the solitary wave solution $\omega = \omega(\hat{\zeta})$ is regular at $\hat{\zeta} = 1$. In this paper, this $\hat{\zeta}$-plane is called Packham's complex plane.

3.3. Packham's solitary wave solution with Davies' approximation. By applying the leading-order approximation of Davies (2.7) to the free surface boundary condition (3.7), Packham [19] obtained a solitary wave solution in the $\hat{\zeta}$-plane:

$$\omega(\hat{\zeta}) = -\frac{1}{3}\log\left\{1-\sin^2\mu\pi\cdot(1-\hat{\zeta})\right\}. \tag{3.9}$$

This is called Packham's approximate solitary wave solution. Note that this solution has a logarithmic singularity at $\hat{\zeta} = -\cot^2\mu\pi$ exterior to the flow domain, and this singular point approaches the crest C on the negative real axis in the $\hat{\zeta}$-plane with the increase of wave amplitude. When this logarithmic singularity reaches the crest C, namely, at $\mu = 1/3$ and the corresponding Froude number $F = (3\sqrt{3}/\pi)^{1/2} \simeq 1.286074$, Packham's approximate solution (3.9) attains the highest wave which has a corner flow with the inner angle of 120 degrees at crest. This behavior of the exterior singularity qualitatively agrees with that of the leading-order singularity of the fully nonlinear solution although the location and the coefficient of the logarithmic singularity are not correct [17, 18].

4. Computation of solitary wave solutions in Packham's complex plane. In this section, we introduce a numerical method to obtain solitary wave solutions satisfying the high-order approximation of Davies (2.9), with which Levi-Civita's surface condition (1.1) in the $\hat{\zeta}$-plane can be approximated, from (3.7), by

$$G_M^{(\mathrm{D})}(\hat{\sigma}) := 2\sin\frac{\hat{\sigma}}{2}\sqrt{\sin^2\frac{\hat{\sigma}}{2}+\tan^2\mu\pi}\,\frac{\partial\tau}{\partial\hat{\sigma}} + \mathrm{e}^{3\tau}\sum_{m=1}^{M}A_m(\sin 3\theta)^{2m-1} = 0 \quad \text{on } \hat{\zeta} = \hat{\rho}(\hat{\sigma})\mathrm{e}^{\mathrm{i}\hat{\sigma}} \quad (0 < \hat{\sigma} < 2\pi). \tag{4.1}$$

The algorithm proposed here is similar to that developed for periodic waves on water of finite depth in [17] but is modified for solitary waves, as follows.

4.1. Polynomial approximation. Since a solitary wave solution ω is analytic in the flow domain and on its boundary Γ in the $\hat{\zeta}$-plane, $\omega = \omega(\hat{\zeta})$ can be expanded in the form of power series. In addition, from the bottom condition and the symmetry condition,

$$\theta = 0 \qquad (-1 < \hat{\zeta} < 1), \tag{4.2}$$

and the infinity condition,

$$\omega(\hat{\zeta}) \ \to \ 0 \qquad (\hat{\zeta} \to 1), \tag{4.3}$$

we can write $\omega = \omega(\hat{\zeta})$ as

$$\omega(\hat{\zeta}) = \sum_{k=1}^{\infty} \hat{b}_k (1 - \hat{\zeta}^k) \qquad (\hat{b}_k \in \mathbb{R}). \tag{4.4}$$

Here it should be noted that the Kth partial sum of the infinite series in (4.4) exactly satisfies the boundary conditions (4.2) and (4.3), and the exponential decay condition with Stokes' relation (1.2) in the outskirt, for any $K = 1, 2, \ldots$. Also any partial sum is regular, and its real part τ and imaginary part θ are both harmonic. Thus we may obtain an approximate solution using a partial sum of (4.4) such that the free surface condition (3.7) or (4.1) is satisfied with sufficient accuracy for relatively small wave amplitudes. Unfortunately, to compute solitary wave solutions of large amplitudes, we have to take another singular point into consideration, which approaches the flow domain with the increase of wave amplitude along the negative axis in the $\hat{\zeta}$-plane, as indicated in section 3.3. This singularity close to the flow domain deteriorates convergence of series for $\omega(\hat{\zeta})$. In order to enlarge the circle of convergence of the power series (4.4), we move the center of expansion from the origin to the midpoint $\hat{\zeta} = \hat{\xi}_1$ between the crest C ($\hat{\zeta} = -\hat{\rho}(\hat{\sigma} = \pi)$) and the physical infinity $\hat{\zeta} = 1$ in the $\hat{\zeta}$-plane and represent $\omega(\hat{\zeta})$ as

$$\omega(\hat{\zeta}) = \sum_{k=1}^{\infty} \tilde{a}_k \left[1 - \{(\hat{\zeta} - \hat{\xi}_1)/\hat{\gamma}_1\}^k \right] \qquad (\tilde{a}_k \in \mathbb{R}), \tag{4.5}$$

where $\hat{\xi}_1 = \{1 - \hat{\rho}(\pi)\}/2$ and $\hat{\gamma}_1 = \{1 + \hat{\rho}(\pi)\}/2$ with $\hat{\rho}(\pi) = \tan^2(\mu\pi/2)$.

Convergence of this infinite series can be further improved using the idea of orthogonalization of basis functions, as discussed in Appendix A. In this work, we transform the basis functions of the infinite series in (4.5) to orthogonal polynomials $\hat{p}_k$'s using the numerical orthogonalization method described in [17], and we write the transformed Kth partial sum in the form of

$$\omega_K(\hat{\zeta}) = \sum_{k=1}^{K} \hat{a}_k \, \hat{p}_k(\hat{\zeta}) \qquad (\hat{a}_k \in \mathbb{R}). \tag{4.6}$$

We may then determine the unknown coefficients $\hat{\boldsymbol{a}} = \{\hat{a}_1, \hat{a}_2, \ldots, \hat{a}_K\}$ using numerical minimization of the mean-square error $E(\hat{\boldsymbol{a}}) = \int_0^{\pi} \{G_M^{(\mathrm{D})}(\hat{\sigma}; \hat{\boldsymbol{a}})\}^2 \mathrm{d}\hat{\sigma}$, where $G_M^{(\mathrm{D})}(\hat{\sigma}; \hat{\boldsymbol{a}})$ is the left-hand side of the approximate free surface condition (4.1) with $\omega_K(\hat{\zeta} = \hat{\rho}\mathrm{e}^{\mathrm{i}\hat{\sigma}}) = \tau_K(\hat{\sigma}) + \mathrm{i}\theta_K(\hat{\sigma})$. For this minimization, we numerically solve the

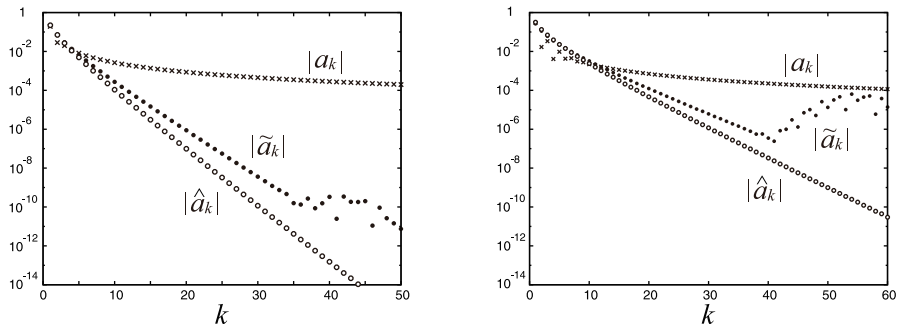

(a) $F = 1.2$ (b) $F = 1.25$

FIG. 3. *Comparison of the absolute values* $|\hat{a}_k|$, $|\tilde{a}_k|$, *and* $|a_k|$ *of coefficients in series expansions of* ω. *White circle* $\circ$: *the coefficient* $\hat{a}_k$ *of the orthogonalized polynomial expansion* (4.6) *in the* $\hat{\zeta}$-*plane; black circle* $\bullet$: *the coefficient* $\tilde{a}_k$ *of the power series* (4.5) *in the* $\hat{\zeta}$-*plane; cross* $\times$: *the coefficient* a_k *of the power series* (4.8) *in the* ζ-*plane.*

simultaneous nonlinear equations $H_k(\hat{\boldsymbol{a}}) = \partial E/\partial \hat{a}_k = \int_0^\pi 2G_M^{(\mathrm{D})}(\partial G_M^{(\mathrm{D})}/\partial \hat{a}_k)\mathrm{d}\hat{\sigma} = 0$ $(k = 1, 2, \ldots, K)$ for the K unknowns $\hat{a}_k$'s using Newton's method

$$\hat{\boldsymbol{a}}^{(\nu+1)} = \hat{\boldsymbol{a}}^{(\nu)} - \left(\frac{\partial \boldsymbol{H}}{\partial \hat{\boldsymbol{a}}}\bigg|_{\hat{\boldsymbol{a}}=\hat{\boldsymbol{a}}^{(\nu)}} \right)^{-1} \boldsymbol{H}(\hat{\boldsymbol{a}}^{(\nu)}) \qquad (\nu = 0, 1, \ldots), \tag{4.7}$$

with a convergence condition of $\|G_M^{(\mathrm{D})}\|_{\max} = \max_{0\le\hat{\sigma}\le\pi} |G_M^{(\mathrm{D})}(\hat{\sigma}; \hat{\boldsymbol{a}})| < 10^{-9}$, where $\boldsymbol{H}(\hat{\boldsymbol{a}}) = (H_1(\hat{\boldsymbol{a}}), H_2(\hat{\boldsymbol{a}}), \ldots, H_K(\hat{\boldsymbol{a}}))$. For that, for small amplitude waves with $F \le 1.1$, we expanded Packham's approximate solution (3.9) in the form of (4.6) and adopted its coefficients as the initial values $\hat{\boldsymbol{a}}^{(0)}$ in (4.7). For large amplitude waves, the initial values $\hat{\boldsymbol{a}}^{(0)}$ are continuously changed with increase of wave amplitude. Then, for sufficiently large number K, the sequence $\{\hat{\boldsymbol{a}}^{(\nu)}\}$ in (4.7) converged fast with ν.

4.2. Fully nonlinear solutions. While there are a number of previous computations of fully nonlinear solitary wave solutions using conformal mapping [2, 5, 10, 13, 24, 25, 26, 29], the numerical method described for high-order Davies' approximate surface condition has been used here for convenience since the method can be equally applied to fully nonlinear surface condition by simply replacing $G_M^{(\mathrm{D})}(\hat{\sigma})$ by $G(\hat{\sigma})$.

In order to demonstrate the effectiveness of the orthogonalization of basis functions, we consider the fully nonlinear case and compare convergence of the unknown coefficients $\hat{a}_k$'s in (4.6) with that of $\tilde{a}_k$'s in (4.5), as shown in Figure 3. This figure also includes the Fourier coefficients a_k's of $\theta = \theta(\sigma)$ in the ζ-plane, where $\theta(\sigma) = -\sum_{k=1}^{\infty} a_k \sin k\sigma$. Here a_k's can be considered as the coefficients of power series expansion of ω in the ζ-plane, which is given by

$$\omega(\zeta) = \sum_{n=1}^{\infty} a_k(1 - \zeta^k) \qquad (a_k \in \mathbb{R}). \tag{4.8}$$

Comparison of convergence of these coefficients in Figure 3 shows that the orthogonalization of basis functions indeed improves convergence and helps us stably catch the high-order terms even for large values of the Froude number F or large wave amplitudes.

TABLE 1

The number K of terms of the partial sums for computation with the convergence condition $\|G^*\|_{\max} < 10^{-9}$. Fully nonlinear computation: $G^* = G$ in (3.7); high-order Davies' approximation of order M: $G^* = G_M^{(\mathrm{D})}$ in (4.1) for $2 \le M \le 5$.

	Fully nonlinear computation	High-order Davies' approximation
$F \le 1.15$	25	20
$1.15 < F \le 1.20$	50	50
$1.20 < F \le 1.25$	65	70
$1.25 < F \le 1.27$	100	110
$1.27 < F \le 1.28$	140	160

Table 1 shows the number K of terms of the partial sum ω_K in (4.6) used for computations for both high-order Davies' approximate and fully nonlinear surface conditions with convergence conditions of $\|G_M^{(\mathrm{D})}\|_{\max} < 10^{-9}$ and $\|G\|_{\max} < 10^{-9}$, respectively.

5. Numerical examples and discussions. In this section, we compare some computed results of the wave profile and the kinetic energy E_{k} of high-order Davies' approximate solutions with those of fully nonlinear solutions for $1 < F \le 1.28$, for which F monotonically changes with wave amplitude. We also apply the weakly and strongly nonlinear long wave approximations to Levi-Civita's surface condition (1.1) in the complex velocity potential f-plane as shown in Appendix B. We should remark that the long wave approximations have previously been applied to the free surface boundary conditions in the physical domain. Then we compute the high-order long wave approximate solutions and compare them with high-order Davies' approximate solutions. Note that τ at the bottom is assumed to be small in the weakly nonlinear long wave approximation but not in the strongly nonlinear one. These computed results are obtained using the method of computation described in section 4 and Appendix B.3.

Using $\tau = \tau(\hat{\sigma})$ and $\theta = \theta(\hat{\sigma})$ on the free surface in the $\hat{\zeta}$-plane and $\mathrm{e}^{-\omega} = \mathrm{d}f/\mathrm{d}z$, we can write the wave profile $(x(\hat{\sigma}), y(\hat{\sigma}))$ of a solitary wave as

$$\left\{\begin{aligned} x(\hat{\sigma}) &= F^2 \int_{\hat{\sigma}}^{\pi} \frac{\mathrm{e}^{\tau}\cos\theta}{2\sin\frac{\hat{\sigma}'}{2}\sqrt{\sin^2\frac{\hat{\sigma}'}{2} + \tan^2\mu\pi}}\mathrm{d}\hat{\sigma}', \\ y(\hat{\sigma}) &= -F^2 \int_{0}^{\hat{\sigma}} \frac{\mathrm{e}^{\tau}\sin\theta}{2\sin\frac{\hat{\sigma}'}{2}\sqrt{\sin^2\frac{\hat{\sigma}'}{2} + \tan^2\mu\pi}}\mathrm{d}\hat{\sigma}', \end{aligned}\right. \tag{5.1}$$

and the wave amplitude-to-depth ratio $\alpha = a/h$ is given by $\alpha = y(\hat{\sigma} = \pi)$. The kinetic energy normalized by $\rho g h^3$ is obtained by

$$E_{\mathrm{k}} = \int_{-\infty}^{\infty}\int_{-1}^{\eta} \frac{F^2}{2}\{(u-1)^2 + v^2\}\,\mathrm{d}y\,\mathrm{d}x = \int_0^{\pi} \frac{F^6}{4}\frac{(\mathrm{e}^{\tau}\cos\theta - 1)(1-\mathrm{e}^{-2\tau})}{\sin\frac{\hat{\sigma}}{2}\sqrt{\sin^2\frac{\hat{\sigma}}{2} + \tan^2\mu\pi}}\mathrm{d}\hat{\sigma}, \tag{5.2}$$

where $\eta = \eta(x)$ denotes the wave elevation. Also the kinetic energy density $\mathrm{d}\hat{E}_{\mathrm{k}}/\mathrm{d}\hat{\sigma}$ along the free surface $\hat{\zeta} = \hat{\rho}\mathrm{e}^{\mathrm{i}\hat{\sigma}}$ in the $\hat{\zeta}$-plane is given by the integrand of the second integral in (5.2), namely,

$$\frac{\mathrm{d}\hat{E}_{\mathrm{k}}}{\mathrm{d}\hat{\sigma}} = \frac{F^6}{4}\frac{(\mathrm{e}^{\tau}\cos\theta - 1)(1-\mathrm{e}^{-2\tau})}{\sin\frac{\hat{\sigma}}{2}\sqrt{\sin^2\frac{\hat{\sigma}}{2} + \tan^2\mu\pi}}. \tag{5.3}$$

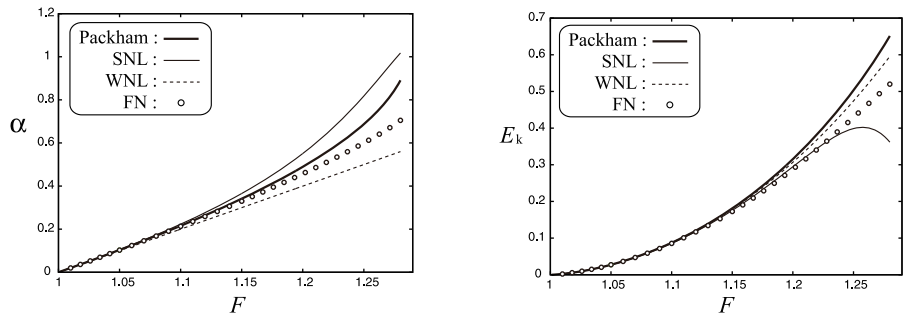

(a) Wave amplitude-to-depth ratio α (b) Kinetic energy E_k

FIG. 4. *Variation of the wave amplitude-to-depth ratio $\alpha = a/h$ and the kinetic energy E_k of the lowest-order approximate solutions with the Froude number F. Thick solid line (Packham): Packham's approximate solution* (3.9) *for $G_M^{(D)}(\hat{\sigma}) = 0$ in* (4.1) *with $M = 1$; thin solid line (SNL): the strongly nonlinear long wave approximate solution for $G_N^{(S)}(\phi) = 0$ in* (B.6) *with $N = 1$; thin dashed line (WNL): the weakly nonlinear long wave approximate solution* (B.15) *for $G_N^{(W)}(\phi) = 0$ in* (B.14) *with $N = 1$; circle ∘ (FN): the fully nonlinear solution.*

5.1. Comparison of the lowest-order approximate solutions. The lowest-order solutions of Davies' approximate equation $G_M^{(D)}(\hat{\sigma}) = 0$ in (4.1) with $M = 1$ and the weakly nonlinear long wave approximate equation $G_N^{(W)}(\phi) = 0$ in (B.14) with $N = 1$ are given by (3.9) and (B.15), respectively. The lowest-order solution of the strongly nonlinear long wave approximate equation $G_N^{(S)}(\phi) = 0$ in (B.6) with $N = 1$ can be numerically obtained using the computational method in section 4 and Appendix B.3. Figures 4(a) and (b) compare variations of the wave amplitude-to-depth ratio $\alpha = a/h$ and the kinetic energy E_k with the Froude number F of these lowest-order approximate and fully nonlinear solutions, respectively. These figures show that all three lowest-order approximate solutions are accurate for $F \leq 1.1$. The computed results of α of the lowest-order solution of Davies' approximation (that was also referred to as Packham's approximate solitary wave solution) are close to those of the fully nonlinear solutions for $F \leq 1.2$ and slightly more accurate than the long wave approximate solutions. The kinetic energy E_k is computed with comparable accuracy by all three approximations for $F \leq 1.2$. However, we should examine these computed results of the integrated values carefully, because the corresponding integrands may be incorrect even if the integrated values are accurate, as shown in Figure 5.

Figure 5 compares the wave profile given by (5.1) and the kinetic energy density $\mathrm{d}\hat{E}_k/\mathrm{d}\hat{\sigma}$ given by (5.3) of the lowest-order approximate solutions for $F = 1.1$, 1.2, and 1.28. Note that $\hat{\sigma}$ represents the location on the free surface $\hat{\zeta} = \hat{\rho}\mathrm{e}^{\mathrm{i}\hat{\sigma}}$ in the $\hat{\zeta}$-plane, as shown in Figure 1(d), and that $\hat{\sigma} = 0$ and $\hat{\sigma} = \pi$ correspond to the physical infinity and the crest, respectively. We can find that the lowest-order solution of Davies' approximation is much more accurate than the long wave approximate solutions except near the crest. In the outskirt of wave, the strongly nonlinear long wave approximate solution is also accurate even for large amplitude waves. Note that the crest of the lowest-order solution of Davies' approximation becomes sharper due to the logarithmic singularity exterior to the flow domain, as described in section 3.3. Also the results of the kinetic energy density $\mathrm{d}\hat{E}_k/\mathrm{d}\hat{\sigma}$ in Figures 4 and 5 indicate that the integrated quantities of approximate solutions can be coincidentally close to the fully nonlinear solutions even if the corresponding integrands are erroneous.

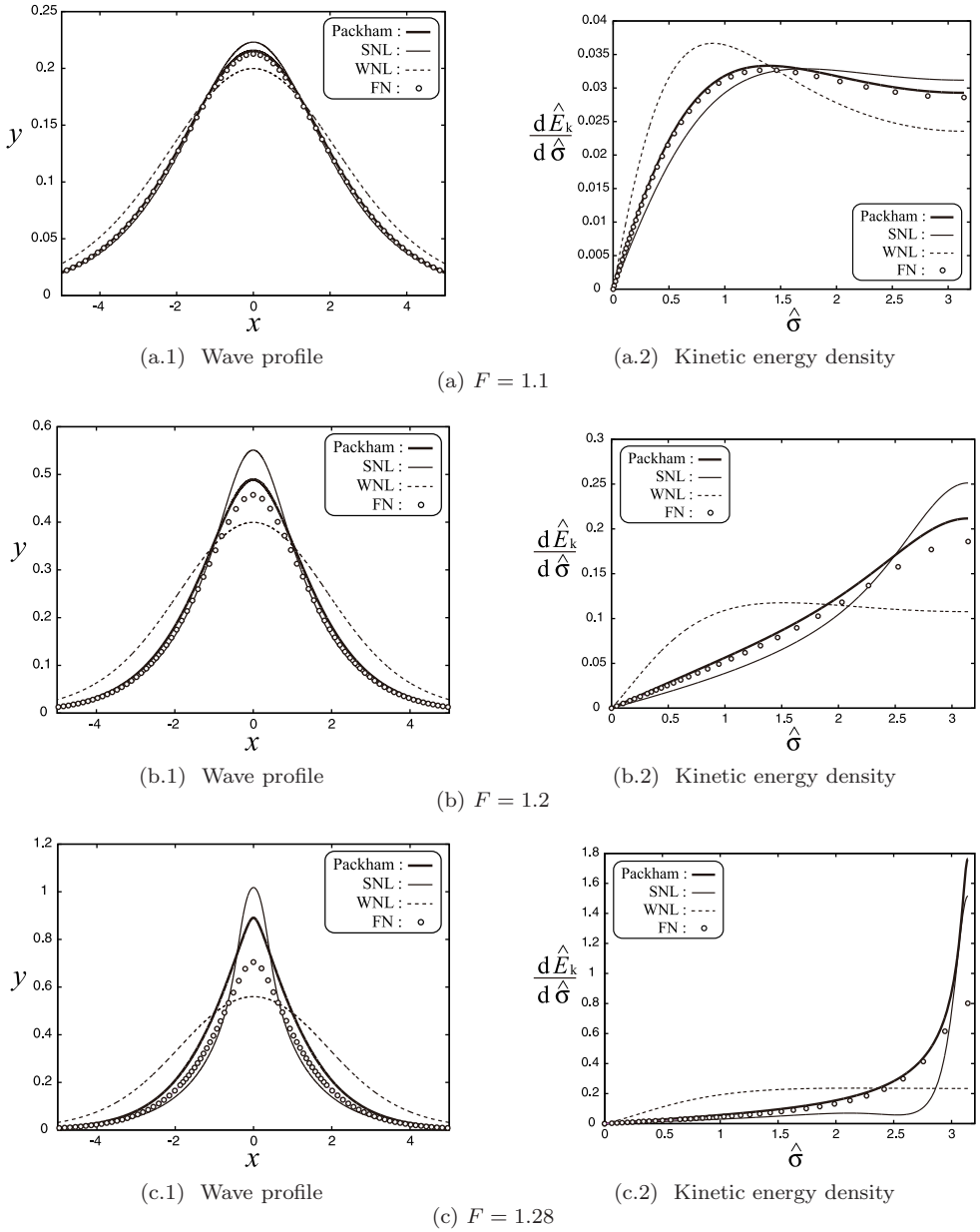

(a.1) Wave profile (a.2) Kinetic energy density

(a) $F = 1.1$

(b.1) Wave profile (b.2) Kinetic energy density

(b) $F = 1.2$

(c.1) Wave profile (c.2) Kinetic energy density

(c) $F = 1.28$

FIG. 5. *Comparison of the wave profile and the kinetic energy density* $\mathrm{d}\hat{E}_\mathrm{k}/\mathrm{d}\hat{\sigma}$ *of lowest-order solutions. The free surface* Γ *in the* $\hat{\zeta}$*-plane is represented by* $\hat{\zeta} = \hat{\rho}\mathrm{e}^{\mathrm{i}\hat{\sigma}}$*, as shown in Figure* 1(d)*, where* $\hat{\sigma} = 0$ *is the physical infinity and* $\hat{\sigma} = \pi$ *is the crest. See caption in Figure* 4.

5.2. Comparison of convergence of the high-order approximate solutions. Figures 6(a) and (b) compare convergence of the wave profile and the kinetic energy density $\mathrm{d}\hat{E}_\mathrm{k}/\mathrm{d}\hat{\sigma}$ of the three high-order approximate solutions to those of fully nonlinear solutions for $F = 1.2$ and 1.28, respectively. It is found that high-order Davies' approximate solutions converge quickly to the fully nonlinear solutions with the order $M = 2$ or 3 even for large amplitude waves, and their convergence rates are much faster than those of the other two long wave approximate solutions. These

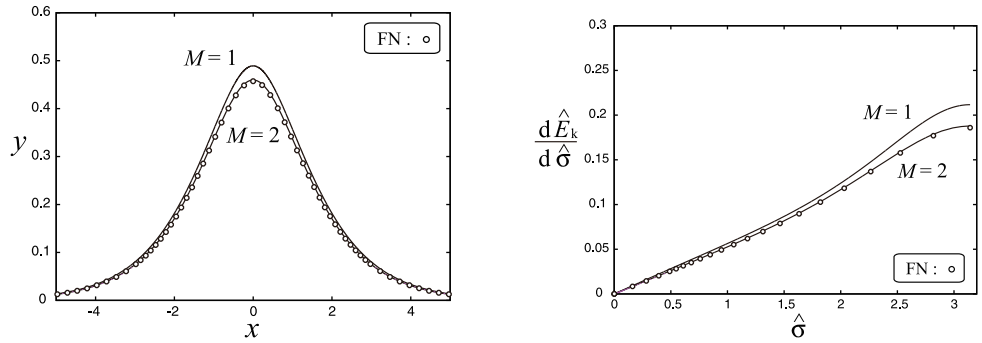

(a.1.1) Wave profile (a.1.2) Kinetic energy density

(a.1) Davies' approximate solutions of order M for $G_M^{(\mathrm{D})}(\hat{\sigma}) = 0$ in (4.1)

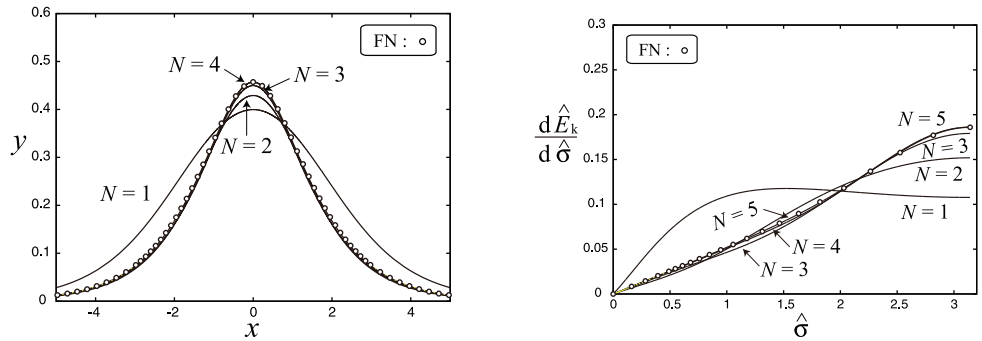

(a.2.1) Wave profile (a.2.2) Kinetic energy density

(a.2) Weakly nonlinear long wave approximate solutions of order N for $G_N^{(\mathrm{W})}(\phi) = 0$ in (B.14)

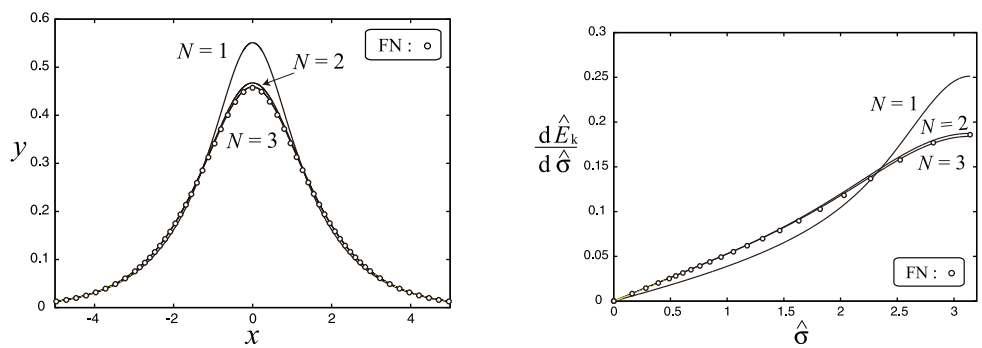

(a.3.1) Wave profile (a.3.2) Kinetic energy density

(a.3) Strongly nonlinear long wave approximate solutions of order N for $G_N^{(\mathrm{S})}(\phi) = 0$ in (B.6)

(a) $F = 1.2$

FIG. 6. *Comparison of the wave profile and the kinetic energy density* $\mathrm{d}\hat{E}_\mathrm{k}/\mathrm{d}\hat{\sigma}$ *of high-order approximate solutions. The free surface* Γ *in the* $\hat{\zeta}$*-plane is represented by* $\hat{\zeta} = \hat{\rho}\mathrm{e}^{\mathrm{i}\hat{\sigma}}$*, as shown in Figure* 1(d)*, where* $\hat{\sigma} = 0$ *is the physical infinity and* $\hat{\sigma} = \pi$ *is the crest. Circle* $\circ$ *(FN): the fully nonlinear solution.*

results imply the importance of the evaluation of the dominant singularities described in sections 3.1 and 3.3 in the approximation of solitary wave solutions, because this evaluation is less accurate in the long wave approximations. Note that the strongly

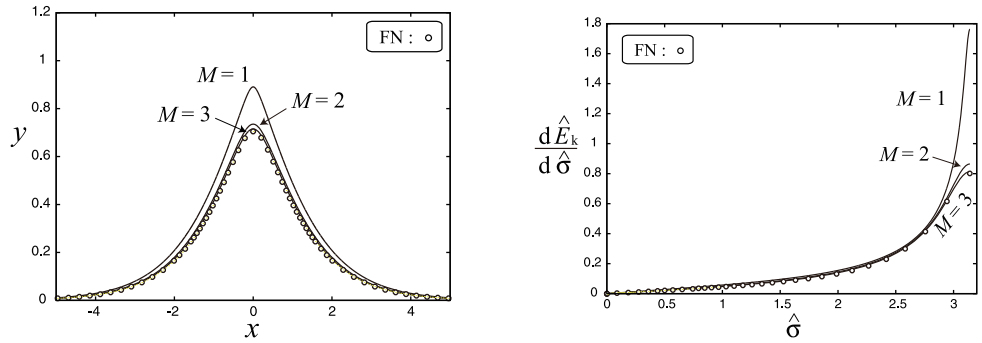

(b.1.1) Wave profile (b.1.2) Kinetic energy density

(b.1) Davies' approximate solutions of order M for $G_M^{(\mathrm{D})}(\hat{\sigma}) = 0$ in (4.1)

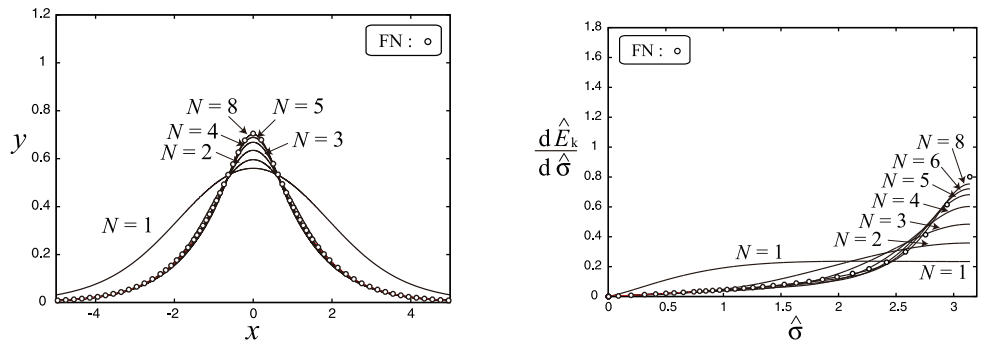

(b.2.1) Wave profile (b.2.2) Kinetic energy density

(b.2) Weakly nonlinear long wave approximate solutions of order N for $G_N^{(\mathrm{W})}(\phi) = 0$ in (B.14)

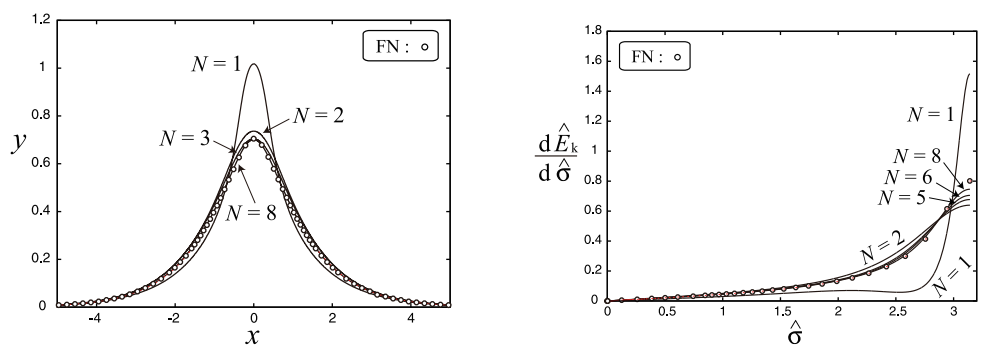

(b.3.1) Wave profile (b.3.2) Kinetic energy density

(b.3) Strongly nonlinear long wave approximate solutions of order N for $G_N^{(\mathrm{S})}(\phi) = 0$ in (B.6)

(b) $F = 1.28$

FIG. 6. *(cont.)*

nonlinear long wave approximate solutions converge faster than the weakly nonlinear ones but slower than high-order Davies' approximate solutions due to poor accuracy of approximation of the singularities for large amplitude waves.

6. Conclusions. We have considered a new type of approximation, high-order Davies' approximation (4.1), to Levi-Civita's free surface condition (1.1) for two-dimensional irrotational motion of a solitary wave progressing in permanent form in

an ideal fluid of constant depth. In comparison with fully nonlinear solitary wave solutions, it is shown that this approximation in Packham's complex plane defined by (3.4) yields rapidly converging series solutions even for relatively large amplitude waves, for which classical long wave approximations fail.

Despite its long history, the solitary wave problem is still challenging to solve due to not only the nonlinearity of the free surface condition but also the exponential decay of the outskirt of a solitary wave solution with Stokes' relation (1.2). Through conformal mapping originally introduced by Packham [19], a singularity of the solution at infinity is regularized so that the solitary wave solution written in the form of power series exactly satisfies the exponential decay condition and the harmonic property.

We have developed an efficient and accurate polynomial approximation with a suitably defined norm using a polynomial system orthogonalized on the free surface. It should be emphasized that the formulation in the conformally mapped plane enables us to examine singularities exterior to the flow domain and obtain rapid convergence of series expansion of a solution.

The numerical method developed here has been used to obtain in Packham's complex plane both high-order Davies' approximate solutions and fully nonlinear solutions for the range of $1 < F \leq 1.28$, where the wave amplitude changes monotonically with the Froude number F. In addition, the high-order weakly and strongly nonlinear long wave approximations to Levi-Civita's surface condition have been presented in Appendix B. Then, we have compared these four solutions, focusing on the wave amplitude-to-depth ratio $\alpha = a/h$, the wave profile, the kinetic energy E_{k}, and the kinetic energy density $\mathrm{d}\hat{E}_{\mathrm{k}}/\mathrm{d}\hat{\sigma}$.

For values of $F \leq 1.1$, Davies' approximate solutions (even with the leading-order approximation or $M = 1$) compare reasonably well with the fully nonlinear and strongly nonlinear long wave solutions while the weakly nonlinear long wave solutions deviate from others even for small values of $F - 1$. As F increases to 1.2, Davies' approximate solutions with $M = 1$ or 2 show better comparison with the fully nonlinear solutions than the strongly nonlinear long wave solutions. In particular, the integrated quantities (such as the kinetic energy and the kinetic energy density) from Davies' approximate solutions show excellent agreement with the fully nonlinear solutions. As F increases further ($F \geq 1.2$), high-order Davies' approximations ($M > 1$) are required, but it is demonstrated that Davies' approximate solutions even with $M = 2$ or 3 converge to fully nonlinear solutions much faster than high-order strongly long wave approximate solutions. From this study, it can be concluded that Davies' approximation is superior to the classical long wave approximations in obtaining steady solitary wave solutions.

Appendix A. Improvement of polynomial approximation in Packham's complex plane. The Kth partial sum of the infinite series in (4.4) is a polynomial of degree K in the $\hat{\zeta}$-plane. The accuracy of polynomial approximation in the $\hat{\zeta}$-plane can be improved as follows. First, in order to examine the accuracy of approximate solutions in the $\hat{\zeta}$-plane, we define the inner product $(\varphi_1, \varphi_2)_\Gamma$ of two complex functions $\varphi_1(\hat{\zeta})$ and $\varphi_2(\hat{\zeta})$ and the norm $\|\varphi_1\|_\Gamma$ by [9, section 18.4]

$$(\mathrm{A.1})\quad (\varphi_1, \varphi_2)_\Gamma = \int_0^{2\pi} \varphi_1(\hat{\zeta} = \hat{\rho}\mathrm{e}^{\mathrm{i}\hat{\sigma}})\, \overline{\varphi_2(\hat{\zeta} = \hat{\rho}\mathrm{e}^{\mathrm{i}\hat{\sigma}})}\, \mathrm{d}\hat{\sigma} \quad \text{and} \quad \|\varphi_1\|_\Gamma = \sqrt{(\varphi_1, \varphi_1)_\Gamma},$$

respectively, where $\overline{\varphi_2(\hat{\zeta})}$ denotes the conjugate of $\varphi_2(\hat{\zeta})$. Then, the following theorem

guarantees that the error of polynomial approximation can be minimized using a polynomial system orthogonalized on the free surface Γ in the $\hat{\zeta}$-plane.

THEOREM A.1 (Henrici [9, Theorem 18.4d, p. 557]). *Let $\omega(\hat{\zeta})$ be analytic in the flow domain and continuous on its boundary Γ in the $\hat{\zeta}$-plane. Then the best approximation of $\omega(\hat{\zeta})$ in the norm $\| \ \|_\Gamma$ by a polynomial of degree $\leq K$ is given by*

$$\omega_K(\hat{\zeta}) = \sum_{k=1}^{K} c_k p_k(\hat{\zeta}) \qquad \text{with } c_k = (\omega, p_k)_\Gamma, \tag{A.2}$$

where p_k's are the orthonormal polynomials satisfying

$$(p_k, p_\ell)_\Gamma = \delta_{k\ell} = \begin{cases} 1 & (k = \ell), \\ 0 & (k \neq \ell). \end{cases} \tag{A.3}$$

We can numerically determine the orthonormal polynomials $p_k(\hat{\zeta})$ in (A.2) using the Gram–Schmidt transformation for linearly independent polynomials in the $\hat{\zeta}$-plane such as $\{1-\hat{\zeta}, 1-\hat{\zeta}^2, 1-\hat{\zeta}^3, \ldots, 1-\hat{\zeta}^N\}$, which are the basis functions of (4.4).

Appendix B. Long wave approximation in the complex velocity potential plane. We can apply a long wave approximation to the flow in the f-plane shown in Figure 1(b) by assuming that high-order derivative terms with respect to ϕ are negligible. Friedrichs and Hyers [8, pp. 521–522] obtained an approximate solution for $\omega = \omega(f)$ by applying the long wave approximation to Levi-Civita's surface condition (1.1) on the weakly nonlinear or small amplitude assumption that τ is small. This assumption for τ is required for approximation of the exponential term $\mathrm{e}^{3\tau}$ in (1.1) using the Taylor expansion. Here, without any assumption on the wave amplitude, we derive a strongly nonlinear long wave approximation by transforming Levi-Civita's surface condition (1.1) for $\omega(f)$ to the condition for $\Omega(f) = \mathrm{e}^{-\omega(f)}$.

B.1. Strongly nonlinear long wave approximation. Introducing a new complex variable $\Omega(f) = \mathrm{e}^{-\omega(f)}$, we can rewrite Levi-Civita's surface condition (1.1) as

$$\frac{\partial}{\partial \phi}\left\{\left({\Omega_\mathrm{r}}^2 + {\Omega_\mathrm{i}}^2\right)^2\right\} - \frac{4}{F^2}\Omega_\mathrm{i} = 0 \quad \text{on} \quad \psi = 0, \tag{B.1}$$

where $\Omega(f) = \Omega_\mathrm{r}(\phi,\psi) + \mathrm{i}\,\Omega_\mathrm{i}(\phi,\psi)$ with $\Omega_\mathrm{r}(\phi,\psi) = \mathrm{e}^{-\tau}\cos\theta$ and $\Omega_\mathrm{i}(\phi,\psi) = -\mathrm{e}^{-\tau}\sin\theta$. Equation (B.1) can be considered as the free surface condition for $\Omega(f) = \mathrm{e}^{-\omega(f)}$ in the f-plane. Since no exponential terms appear in (B.1), the weakly nonlinear assumption is not necessary for the long wave approximation of (B.1). Under the bottom condition $\Omega_\mathrm{i} = 0$ at $\psi = -1$, $\Omega = \Omega(f)$ can be expanded around the bottom in the f-plane as

$$\Omega(f) = \sum_{n=0}^{\infty} \frac{1}{n!}\left[\{\mathrm{i}(\psi+1)\}^n \frac{\mathrm{d}^n}{\mathrm{d}\phi^n}\right]\check{\Omega}_\mathrm{r}(\phi) = \mathrm{e}^{\mathrm{i}(\psi+1)\frac{\mathrm{d}}{\mathrm{d}\phi}}\check{\Omega}_\mathrm{r}(\phi), \tag{B.2}$$

where $\check{\Omega}_\mathrm{r}(\phi)$ is Ω_r evaluated at the bottom, namely, $\check{\Omega}_\mathrm{r}(\phi) = \Omega_\mathrm{r}(\phi, \psi = -1)$. Using (B.2), we can write Ω_r and Ω_i at the surface $\psi = 0$ as

$$\Omega_\mathrm{r}(\phi, \psi = 0) = \sum_{n=0}^{\infty} \frac{(-1)^n}{(2n)!}\mathrm{D}^{2n}\check{\Omega}_\mathrm{r}(\phi) = \cos\mathrm{D}\cdot\check{\Omega}_\mathrm{r} \tag{B.3}$$

and

$$\Omega_{\mathrm{i}}(\phi, \psi = 0) = \sum_{n=0}^{\infty} \frac{(-1)^n}{(2n+1)!} \mathrm{D}^{2n+1} \check{\Omega}_{\mathrm{r}}(\phi) = \sin \mathrm{D} \cdot \check{\Omega}_{\mathrm{r}}, \tag{B.4}$$

respectively, where D is the differential operator defined by $\mathrm{D} = \mathrm{d}/\mathrm{d}\phi$. In the long wave approximation, we can assume

$$\mathrm{D}^n \check{\Omega}_{\mathrm{r}} = \mathrm{O}(\epsilon^n) \qquad (n = 1, 2, \ldots), \tag{B.5}$$

where ϵ is a small parameter of order h/λ, and h and λ denote the water depth and the horizontal scale of wave, respectively. In this approximation, substituting (B.3) and (B.4) into (B.1) and collecting the terms up to the order of $\mathrm{D}^{2N+1}\check{\Omega}_{\mathrm{r}}$ $(= \mathrm{O}(\epsilon^{2N+1}))$ produce

$$G_N^{(\mathrm{S})}(\phi) := \left[\mathrm{D} \left\{ \left((\cos \mathrm{D} \cdot \check{\Omega}_{\mathrm{r}})_N{}^2 + (\sin \mathrm{D} \cdot \check{\Omega}_{\mathrm{r}})_N{}^2 \right)^2 \right\} \right]_N - \frac{4}{F^2} (\sin \mathrm{D} \cdot \check{\Omega}_{\mathrm{r}})_N = 0, \tag{B.6}$$

where $[\,\cdot\,]_N$ denotes truncation of higher-order terms than $\mathrm{D}^{2N+1}\check{\Omega}_{\mathrm{r}}$ in the bracket. We call $G_N^{(\mathrm{S})}(\phi) = 0$ in (B.6) the strongly nonlinear long wave approximate equation. This kind of strongly nonlinear approximation has been applied to solitary waves in the physical plane as described in section 1, but not in the conformally mapped plane such as the f-plane.

The asymptotic behavior of $\check{\Omega}_{\mathrm{r}}(\phi)$ as $\phi \to \pm\infty$ can be assumed to exponentially decay as

$$\check{\Omega}_{\mathrm{r}}(\phi) \ \sim \ 1 + d_1 \, \mathrm{e}^{\mp 2\beta\phi} \qquad (\phi \to \pm\infty), \tag{B.7}$$

where d_1 is a real constant. Substituting this into (B.6) yields an equation for β as

$$2\beta (\cos 2\beta)_N = (\sin 2\beta)_N / F^2. \tag{B.8}$$

This approximates Stokes' relation (1.2) and determines the exponential decay parameter β in (B.7) for given F and N. Note that if F is fixed, the exponential decay rate 2β approaches $\mu\pi$ as $N \to \infty$.

The idea of Packham's complex plane in section 3 can be applied to expand $\check{\Omega}_{\mathrm{r}}$ in a suitable form for numerical computations. First, for an analytic solution Ω_β exponentially decaying with the rate 2β as in (B.7), we can introduce a new complex plane, the $\hat{\zeta}_\beta$-plane, defined by

$$\hat{\zeta}_\beta = \tanh^2 \{\beta(f + \mathrm{i})\} \qquad \text{or} \qquad f + \mathrm{i} = \frac{1}{2\beta} \log \left(\frac{1 + \sqrt{\hat{\zeta}_\beta}}{1 - \sqrt{\hat{\zeta}_\beta}} \right). \tag{B.9}$$

In the $\hat{\zeta}_\beta$-plane, the free surface is mapped onto $\Gamma_\beta : \hat{\zeta}_\beta = \hat{\rho}_\beta(\hat{\sigma}_\beta)\mathrm{e}^{\mathrm{i}\hat{\sigma}_\beta}$, where $\hat{\rho}_\beta(\hat{\sigma}_\beta)$ is given by (3.5) when $\mu\pi$ is replaced by 2β. For numerical calculation of the strongly nonlinear long wave approximate equation (B.6), it is convenient to utilize the $\hat{\zeta}_\beta$-plane. Similarly to (4.4), Ω_β can be expanded in the form

$$\Omega_\beta(\hat{\zeta}_\beta) = 1 + \sum_{k=1}^{\infty} a_{\beta,k} (1 - \hat{\zeta}_\beta)^k \qquad (a_{\beta,k} \in \mathbb{R}). \tag{B.10}$$

Since $\psi = -1$ or $\hat{\zeta}_\beta = \tanh^2(\beta\phi)$ $(0 \le \hat{\zeta}_\beta < 1)$ on the bottom, it may be natural to approximate $\check{\Omega}_{\mathrm{r}}(\phi)$ by the Kth partial sum of (B.10) as

$$\check{\Omega}_{\mathrm{r}}(\phi) \ \sim\ 1 + \sum_{k=1}^{K} a_k^{(\mathrm{S})} \operatorname{sech}^{2k}(\beta\phi) \qquad (a_k^{(\mathrm{S})} \in \mathbb{R}). \tag{B.11}$$

B.2. Weakly nonlinear long wave approximation. The logarithmic hodograph variable $\omega = \omega(f)$ can be expanded around the bottom in the f-plane, similarly to (B.2), and we can write τ and θ at the free surface $\psi = 0$ as

$$\tau(\phi, \psi = 0) = \cos \mathrm{D} \cdot \check{\tau} \quad \text{and} \quad \theta(\phi, \psi = 0) = \sin \mathrm{D} \cdot \check{\tau}, \tag{B.12}$$

where $\cos \mathrm{D}$ and $\sin \mathrm{D}$ are defined in (B.3) and (B.4), respectively, and $\check{\tau}(\phi)$ is τ evaluated at the bottom, namely, $\check{\tau}(\phi) = \tau(\phi, \psi = -1)$. The exponential term $\mathrm{e}^{3\tau} = \mathrm{e}^{3(\cos \mathrm{D} \cdot \check{\tau})}$ of Levi-Civita's surface condition (1.1) can be approximated on the assumption that $\check{\tau}$ is small. For long wave approximation with this weakly nonlinear assumption, we set the orders of $\check{\tau}$ and $\mathrm{D}^n \check{\tau}$ as

$$\check{\tau} = \mathrm{O}(\epsilon^2) \quad \text{and} \quad \mathrm{D}^n \check{\tau} = \mathrm{O}(\epsilon^{n+2}) \qquad (n = 1, 2, \ldots), \tag{B.13}$$

where ϵ is the same small parameter as that in (B.5). Then we can get the following approximate equation by substituting (B.12) into Levi-Civita's surface condition (1.1) and collecting the terms up to the order of $\mathrm{D}^{2N+1}\check{\tau}$ $(= \mathrm{O}(\epsilon^{2N+3}))$:

$$G_N^{(\mathrm{W})}(\phi) := \left[\left(\sum_{n=0}^{\infty} \frac{\{-3(\cos \mathrm{D} \cdot \check{\tau})_N\}^n}{n!} \right) \mathrm{D}(\cos \mathrm{D} \cdot \check{\tau})_N - \frac{1}{F^2} \sin(\sin \mathrm{D} \cdot \check{\tau})_N \right]_N = 0, \tag{B.14}$$

where $[\,\cdot\,]_N$ is defined in (B.6). We call $G_N^{(\mathrm{W})}(\phi) = 0$ in (B.14) the weakly nonlinear long wave approximate equation of order N. For the lowest-order with $N = 1$, integrating twice (B.14) with respect to ϕ, we can obtain a solution as

$$\check{\tau}(\phi) = \frac{F^2 - 1}{F^2} \operatorname{sech}^2 \left(\frac{1}{2} \sqrt{\frac{3(F^2 - 1)}{1 + \frac{3}{2}(F^2 - 1)}} \cdot \phi \right). \tag{B.15}$$

Note that, from this lowest-order approximate solution and $\mathrm{e}^{-\omega} = \mathrm{d}f/\mathrm{d}z$, we can derive the approximate wave profile $\eta = \eta(x)$ in the physical plane, which is equivalent to the solitary wave solution of the KdV equation.

Similarly to (B.7), $\check{\tau}(\phi)$ decays exponentially as $\check{\tau}(\phi) \sim d_2\, \mathrm{e}^{\mp 2\beta\phi}$ $(\phi \to \pm\infty)$, where d_2 and β are both positive constants and β satisfies (B.8). Also, similarly to (B.11), $\check{\tau}(\phi)$ can be approximated as

$$\check{\tau}(\phi) \ \sim\ \sum_{k=1}^{K} a_k^{(\mathrm{W})} \operatorname{sech}^{2k}(\beta\phi) \qquad (a_k^{(\mathrm{W})} \in \mathbb{R}), \tag{B.16}$$

and we can utilize the $\hat{\zeta}_\beta$-plane defined by (B.9) for numerical calculation of the weakly nonlinear long wave approximate equation (B.14).

B.3. The method of computation. When the Froude number F and the order N of long wave approximate equations $G_N^{(\mathrm{W})}(\phi) = 0$ in (B.14) and $G_N^{(\mathrm{S})}(\phi) = 0$ in (B.6) are given, we can numerically fix the value of β satisfying approximate Stokes' relation (B.8). With this value of β, $\check{\tau}(\phi)$ and $\check{\Omega}_{\mathrm{r}}(\phi)$ are approximated by the Kth partial sums in (B.16) and in (B.11), respectively. Then, in the $\hat{\zeta}_\beta$-plane, we can apply the algorithm in section 4.2 to these approximate equations by changing $\mu\pi$ to 2β and G to $G_N^{(\mathrm{W})}$ or $G_N^{(\mathrm{S})}$. Note that the basis functions $\{\mathrm{sech}^{2k}(\beta\phi)\}_{k=1}^K$ in (B.16) or (B.11) are numerically orthogonalized on the free surface Γ_β in the $\hat{\zeta}_\beta$-plane. We can also obtain the wave profile, the kinetic energy, and its density by changing $\mu\pi$ to 2β in (5.1), (5.2), and (5.3), respectively.

REFERENCES

[1] J. G. B. Byatt-Smith, *An exact integral equation for steady surface waves*, Proc. R. Soc. Lond. A, 315 (1970), pp. 405–418.

[2] D. Clamond and D. Dutykh, *Fast accurate computation of the fully nonlinear solitary surface gravity waves*, Comput. & Fluids, 84 (2013), pp. 35–38.

[3] T. V. Davies, *The theory of symmetrical gravity waves of finite amplitude.* I, Proc. R. Soc. Lond. A, 208 (1951), pp. 475–486.

[4] T. V. Davies, *Gravity waves of finite amplitude.* III. *Steady, symmetrical, periodic waves in a channel of finite depth*, Quart. Appl. Math., 10 (1952), pp. 57–67.

[5] D. Dutykh and D. Clamond, *Efficient computation of steady solitary gravity waves*, Wave Motion, 51 (2014), pp. 86–99.

[6] W. A. B. Evans and M. J. Ford, *An exact integral equation for solitary waves (with new numerical results for some "internal" properties)*, Proc. R. Soc. Lond. A, 452 (1996), pp. 373–390.

[7] J. Fenton, *A ninth-order solution for the solitary wave*, J. Fluid Mech., 53 (1972), pp. 257–271.

[8] K. O. Friedrichs and D. H. Hyers, *The existence of solitary waves*, Comm. Pure Appl. Math., 7 (1954), pp. 517–550.

[9] P. Henrici, *Applied Computational Complex Analysis*, Vol. 3, John Wiley & Sons, New York, 1986.

[10] J. K. Hunter and J.-M. Vanden-Broeck, *Accurate computations for steep solitary waves*, J. Fluid Mech., 136 (1983), pp. 63–71.

[11] D. J. Korteweg and G. de Vries, *On the change of form of long waves advancing in a rectangular channel, and on a new type of long stationary waves*, Phil. Mag., 39 (1895), pp. 422–443.

[12] H. Lamb, *Hydrodynamics*, 6th ed., Dover, Mineola, NY, 1945.

[13] C. W. Lenau, *The solitary wave of maximum amplitude*, J. Fluid Mech., 26 (1966), pp. 309–320.

[14] R. R. Long, *Solitary waves in the one- and two-fluid systems*, Tellus, 8 (1956), pp. 460–471.

[15] M. S. Longuet-Higgins and J. D. Fenton, *On the mass, momentum, energy and circulation of a solitary wave.* II, Proc. R. Soc. Lond. A., 340 (1974), pp. 471–493.

[16] L. M. Milne-Thomson, *Theoretical Hydrodynamics*, 5th ed., Dover, Mineola, NY, 1968.

[17] S. Murashige, *Numerical use of exterior singularities for computation of gravity waves in shallow water*, J. Engrg. Math., 77 (2012), pp. 1–18.

[18] S. Murashige, *Davies' surface condition and singularities of deep water waves*, J. Engrg. Math., 85 (2014), pp. 19–34.

[19] B. A. Packham, *The theory of symmetrical gravity waves of finite amplitude.* I. *The solitary wave*, Proc. R. Soc. Lond. A, 213 (1952), pp. 234–249.

[20] S. A. Pennell and C. H. Su, *A seventeenth-order series expansion for the solitary wave*, J. Fluid Mech., 149 (1984), pp. 431–443.

[21] S. A. Pennell, *On a series expansion for the solitary wave*, J. Fluid Mech., 179 (1987), pp. 557–561.

[22] G. G. Stokes, *The outskirts of the solitary wave*, Math. and Phys. Papers, 5 (1905), p. 163.

[23] J, Strutt (Lord Rayleigh), *On waves*, Phil. Mag. 5th Ser., 1 (1876), pp. 257–279.

[24] M. Tanaka, *The stability of solitary waves*, Phys. Fluids, 29 (1986), pp. 650–655.

[25] J.-M. Vanden-Broeck, *Gravity-Capillary Free-Surface Flows*, Cambridge University Press, Cambridge, UK, 2010.

[26] T. Y. Wu, J. Kao, and J. E. Zhang, *A unified intrinsic functional expansion theory for solitary waves*, Acta Mech Sin., 21 (2005), pp. 1–15.

[27] T. Y. Wu, X. Wang, and W. Qu, *On solitary waves. Part 2: A unified perturbation theory for higher order waves*, Acta Mech Sin., 21 (2005), pp. 515–530.

[28] T. Y. Wu and S. Murashige, *On tsunami and the regularized solitary wave theory*, J. Engrg. Math., 70 (2011), pp. 137–146.

[29] H. Yamada, *On the highest solitary wave*, Rep. Res. Inst. Appl. Mech. Kyushu Univ., 5 (1957), pp. 53–67.